Ruthenium carbonyl cluster complexes with oxygen ligands. Reactions between $Ru_3(CO)_{12}$ and 4-methoxyphenol or 2-naphthol. Crystal structure of $Ru_4(\mu_3\text{-}OC_6H_4OMe\text{-}4)_2(\mu\text{-}Cl)(\mu\text{-}OC_6H_4OMe\text{-}4)(CO)_{10}$, an unusual mixed-valence cluster complex

Tyrone P. Jeynes, Marie P. Cifuentes and Mark G. Humphrey *

Department of Chemistry, The University of New England, Armidale, NSW 2351 (Australia)

George A. Koutsantonis and Colin L. Raston

Faculty of Science and Technology, Griffith University, Nathan, Qld 4111 (Australia)

(Received September 29, 1993)

Abstract

The reaction between 4-methoxyphenol and $Ru_3(CO)_{12}$ in cyclohexane has been investigated and found to afford a hexaruthenium 'raft' cluster $Ru_6(\mu\text{-}H)_2(\mu_5\text{-}\eta^7\text{-}OC_6H_3OMe\text{-}4)(CO)_{16}$ (**3a**), together with tetraruthenium clusters incorporating three ($Ru_4(\mu_3\text{-}OC_6H_4OMe\text{-}4)_2(\mu\text{-}Cl)(\mu\text{-}OC_6H_4OMe\text{-}4)(CO)_{10}$ (**3b**)) or four ($Ru_4(\mu_3\text{-}OC_6H_4OMe\text{-}4)_2(\mu\text{-}OC_6H_4OMe\text{-}4)_2(CO)_{10}$ (**3c**)) aryloxo ligands; similarly, reaction of $Ru_3(CO)_{12}$ with 2-naphthol afforded the analogous $Ru_6(\mu\text{-}H)_2(\mu_5\text{-}\eta^7\text{-}OC_{10}H_6)(CO)_{16}$ (**4a**), $Ru_4(\mu_3\text{-}OC_{10}H_7)_2(\mu\text{-}Cl)(\mu\text{-}OC_{10}H_7)(CO)_{10}$ (**4b**) and $Ru_4(\mu_3\text{-}OC_{10}H_7)_2(\mu\text{-}OC_{10}H_7)_2(CO)_{10}$ (**4c**). The source of chloride in **3b** and **4b** is believed to be carbon tetrachloride contaminant in the cyclohexane. An X-ray diffraction study reveals that **3b** contains an $Ru_3(CO)_8$ unit linked to an $Ru(CO)_2$ moiety by two asymmetric triply-bridging and one asymmetric doubly-bridging 4-methoxyphenoxo ligands, and an asymmetric doubly-bridging chloro ligand; this interaction is strongly suggestive of a higher oxidation state ruthenium linked to a trinuclear cluster of formally zero oxidation state. The dynamic ^{13}C NMR spectra of **4c** have been recorded, and are consistent with restricted rotation about the Ar–O linkage of the μ_2-coordinated naphthoxo ligands at low temperature.

Key words: Ruthenium; Carbonyl; Clusters; Phenols; Crystal structure; Fluxionality

1. Introduction

A great deal of interest has been shown recently in modelling the hydrodesulfurization of liquid fuels. Coal-derived fuels contain substantial N- and O-containing contaminants, in addition to the S-containing impurities prevalent in oil. We have been examining the chemistry of ruthenium clusters with small N- and O-donor molecules in order to model the hydrotreating processes, and have recently reported the reactivity of triruthenium clusters towards pyridine [1,2] and piperidine [3]. The most persistent oxygen-containing impurities in coal-derived fuels are phenols and furans [4]. We herein report our initial investigations in this area, using substituted phenols. Reaction products with phenols in various coordination modes should model chemisorbed phenol on the catalyst surface, and the subsequent hydrogenation chemistry of these products should model hydrotreating pathways.

Relatively few ruthenium carbonyl clusters containing O-donor ligands are known [5,6]; in most cases as stated by Bruce [5], the harsh reaction conditions employed led to break-up of the first-formed cluster products. Recently, the reaction between $Ru_3(CO)_{12}$ (**1**) and phenol was examined independently by two groups [7,8]; it afforded the raft cluster $Ru_6(\mu\text{-}H)_2(\mu_5\text{-}\eta^7\text{-}OC_6H_4)(CO)_{16}$ (**2a**) in moderate yield. In subsequent work the carbonylation of **2a** was examined, and found

Correspondence to: Dr. M.G. Humphrey.

* Present address: Department of Chemistry, Australian National University, Canberra, ACT 0200, Australia.

0022-328X/94/$7.00
SSDI 0022-328X(93)24372-C

to regenerate **1** [9]; phosphite substitution on **2a** gave $Ru_6(\mu\text{-}H)_2(\mu_5\text{-}\eta^7\text{-}OC_6H_4)(CO)_{15}\{P(OMe)_3\}$. We have investigated the reactions between **1** and 4-methoxyphenol or 2-naphthol in refluxing cyclohexane, and have found that they yield complex mixtures that include tetraruthenium clusters with three or four aryloxo ligands, as well as analogues of **2a**.

2. Results and discussion

2.1. Synthesis and characterization

The reaction of **1** with 10 molar equivalents of 4-methoxyphenol in refluxing cyclohexane afforded a mixture of products (Scheme 1); chromatographic work-up afforded the known (hydrido)cluster carbonyls $Ru_4(\mu\text{-}H)_4(CO)_{12}$ (9%) and $Ru_4(\mu\text{-}H)_2(CO)_{13}$ (2%), the previously reported (hydrido)cluster carbonyl anion $[Ru_6(\mu_6\text{-}H)(CO)_{18}]^-$ (1%), together with the new clusters $Ru_6(\mu\text{-}H)_2(\mu_5\text{-}\eta^7\text{-}OC_6H_3OMe\text{-}4)(CO)_{16}$ (**3a**) (35%), $Ru_4(\mu_3\text{-}OC_6H_4OMe\text{-}4)_2(\mu\text{-}Cl)(\mu\text{-}OC_6H_4OMe\text{-}4)(CO)_{10}$ (**3b**) (4%) and $Ru_4(\mu_3\text{-}OC_6H_4OMe\text{-}4)_2(\mu\text{-}OC_6H_4OMe\text{-}4)_2(CO)_{10}$ (**3c**) (4%), and other, so far unidentified, products.

The hexaruthenium cluster **3a** was characterized by the usual spectroscopic means. The IR spectrum contains a band at 1811 cm^{-1} assigned to a bridging carbonyl, in addition to terminal carbonyl absorptions. The ^1H NMR spectrum contains two sets of resonances in the ratio 2:1 for edge-bridging (−11.88 (major isomer), −12.72 (minor isomer) ppm) and face-capping (−21.86, −22.36 ppm) hydrides, and methoxy protons (3.69, 3.70 ppm), indicating the presence of isomers, as well as signals due to the aryl protons lying between 6.61 and 3.43 ppm. The phenoxy analogue **2a** was obtained as a 9:1 ratio of isomers, although the form of this isomerism has not been established with certainty [7]. Experiments directed at clarifying the nature of this isomerism are detailed below. The FAB mass spectrum contains a molecular ion at 1179 mass units followed by successive loss of 13 CO ligands.

Complex **3b** was characterized as $Ru_4(\mu_3\text{-}OC_6H_4OMe\text{-}4)_2(\mu\text{-}Cl)(\mu\text{-}OC_6H_4OMe\text{-}4)(CO)_{10}$ on the basis of spectroscopic data and a single-crystal X-ray diffraction study. The IR spectrum is indicative of all-terminal carbonyl coordination and the NMR data are consistent with the presence of three 4-methoxyphenoxo ligands in two different environments. The ^1H NMR spectrum contains two signals due to methoxy protons in the ratio 2 (3.84 ppm):1 (3.80 ppm). The phenyl protons at 7.82 (4H) and 6.95 ppm (4H) were assigned to the *ortho* and *meta* protons of the μ_3-methoxyphenoxo ligands respectively, whilst the complex multiplet found at 7.00 ppm (4H) was assigned to the protons of the μ_2-bound ligand. No resonances arising from hydrido ligands were found. The ^{13}C NMR spectrum contains six signals in the metal-bound carbonyl region, in the ratio 2:2:2:2:1:1 (low field to high field), together with three signals at 158–152 ppm assigned to the *ipso* carbons and four (120–114 ppm) due to *ortho* and *meta* carbons of the organic moieties; in addition, two signals in the ratio 1:2 are present, corresponding to the methoxy carbons. The FAB mass spectrum contains a molecular ion at 1090 mass units, consistent with the formulation $Ru_4(OC_6H_4OMe)_3(Cl)(CO)_{10}$, and confirmed by satisfactory microanalyses. Attempts to ascertain the source of the chloro ligand are given below.

Complex **3c** was identified as $Ru_4(\mu_3\text{-}OC_6H_4OMe\text{-}4)_2(\mu\text{-}OC_6H_4OMe\text{-}4)_2(CO)_{10}$, conceptually related to **3b** by replacement of the chloro ligand by a fourth methoxyphenoxo group. Thus the IR spectrum contains eight bands in the terminal carbonyl region, suggesting that **3c** has a more symmetric structure than the tris-phenoxy cluster (which has nine bands in its IR spectrum). The ^1H and ^{13}C NMR spectra are similar to those of **3b**, but indicative of two equally populated 4-methoxyphenoxo environments. Resonances are found in the ^1H NMR spectrum at 3.80 and 3.79 ppm, corresponding to methoxy groups. The phenyl region contains signals at 7.64 ppm (4H) and 6.85 (4H) assigned to the *ortho* and *meta* protons of the μ_3-bound ligand and a complex multiplet at 6.75 (8H) due to the μ_2-bound ligand. As with **3b**, no hydrido signal was found. The ^{13}C NMR spectrum contains four resonances in the carbonyl region, in the ratio 4:2:2:2 (low field to high field), together with four signals due to the *ipso*-carbons (159–152 ppm) and four signals due to *ortho* and *meta* carbons (120–114 ppm) of the organic ligands; two signals at 55.6 and 55.4 ppm are assigned to methoxy groups. The FAB MS contains a molecular ion at 1178, consistent with the formulation $Ru_4(OC_6H_4OMe)_4(CO)_{10}$.

The reaction between **1** and 2-naphthol proceeded similarly to afford an analogous mixture of products. Thus the 'raft' cluster $Ru_6(\mu\text{-}H)_2(\mu_5\text{-}\eta^7\text{-}OC_{10}H_6)(CO)_{16}$ (**4a**) was obtained in 10% yield as two isomers in a 4:1 ratio; noteworthy is the ^1H NMR spectrum, which clearly indicates differing environments for the protons on the free (7.84–7.36 ppm) and metallated (5.04–4.56 ppm) aromatic rings. Complexes $Ru_4(\mu_3\text{-}OC_{10}H_7)_2(\mu\text{-}Cl)(\mu\text{-}OC_{10}H_7)(CO)_{10}$ (**4b**) and $Ru_4(\mu_3\text{-}OC_{10}H_7)_2(\mu\text{-}OC_{10}H_7)_2(CO)_{10}$ (**4c**) were isolated in 8% and 10% yields, respectively. General features of the spectra are similar to those of the 4-methoxyphenoxo complexes **3b** and **3c**, respectively. Unlike that of **3c**, the room temperature ^{13}C NMR spectrum of **4c** is indicative of dynamic behaviour; this is discussed later after an examination of the crystal structure of **3b**.

Reactions of **1** with other substituted phenols were uniformly unsuccessful. Thus, reaction with 1-naphthol afforded $Ru_4(\mu\text{-}H)_4(CO)_{12}$ (16%) and $Ru_4(\mu\text{-}H)_2(CO)_{13}$ (8%), reaction with 4-ethylphenol gave $Ru_4(\mu\text{-}H)_4(CO)_{12}$ (20%) and reaction with 3,5-dimethylphenol yielded $Ru_4(\mu\text{-}H)_4(CO)_{12}$ (11%) and $Ru_4(\mu\text{-}H)_2(CO)_{13}$ (13%); in none of these reactions were complexes bearing substituted-phenol-derived ligands obtained.

2.2. X-Ray structural study of 3b

As the spectroscopic data do not unequivocally establish the structure of **3b**, a single-crystal X-ray

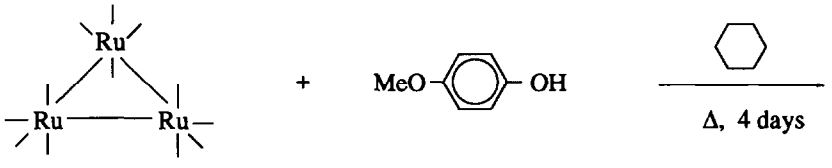

$Ru_4(\mu\text{-}H)_4(CO)_{12}$

$Ru_4(\mu\text{-}H)_2(CO)_{13}$

$[Ru_6(\mu_6\text{-}H)(CO)_{18}]^-$

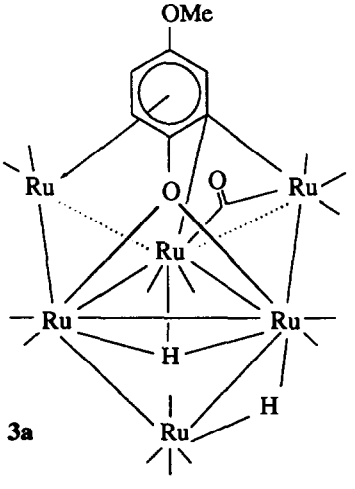

3a

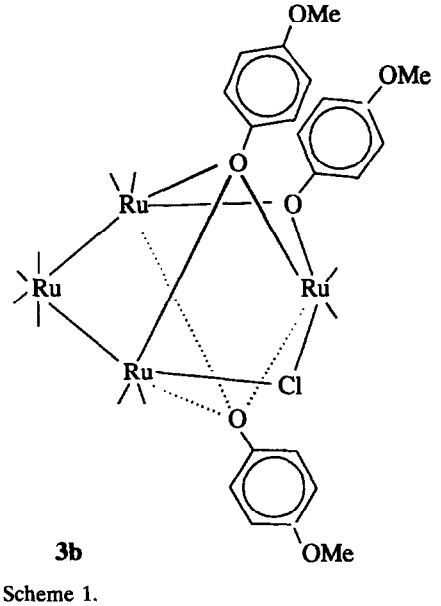

3b

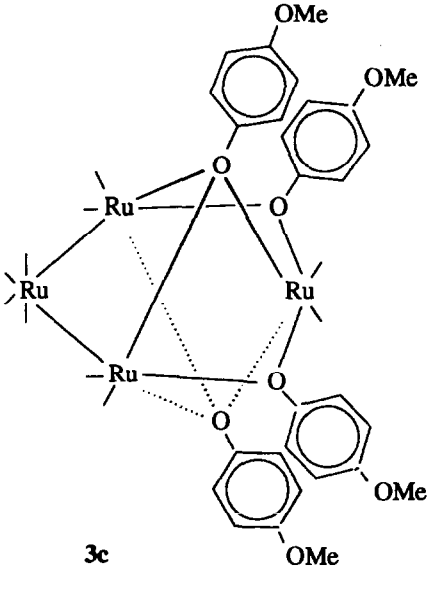

3c

Scheme 1.

diffraction study was carried out. The solid-state structure is shown in Fig. 1; crystallographic data are given in Table 1, atomic coordinates are listed in Table 2, selected bond and contact lengths in Table 3 and selected bond angles in Table 4. Two independent molecules were located in the asymmetric unit, related by minor rotations in the μ_3-OC_6H_4OMe-4 ligands; the two molecules have similar geometries and in the ensuing discussion only one of the molecules is considered. The X-ray study shows that the molecule contains an $Ru_3(CO)_8$ unit linked to an $Ru(CO)_2$ moiety by two asymmetric (μ_3-OC_6H_4OMe-4) and one asymmetric (μ-OC_6H_4OMe-4) ligands and an asymmetric chloro ligand. The Ru(1)–Ru(3) and Ru(2)–Ru(3) distances [av. 2.75 Å] are the only Ru–Ru bonds in the molecule; Ru(1)–Ru(2) (3.12 Å), Ru(1)–Ru(4) (3.09 Å) and Ru(2)–Ru(4) (3.13 Å) are too long for direct Ru–Ru interaction. The CO ligands bound to Ru(1), Ru(2) and Ru(4) have Ru–C distances [av. 1.84 Å] substantially shorter than those of the CO ligands bound to Ru(3) [av. 1.94 Å] as expected; the four CO ligands attached to Ru(3) are in competition for back-bonding. Distances within the 4-methoxyphenoxo ligands are unexceptional. The four rutheniums and bridging oxygen and chlorine ligands define a plane, the maximum deviation from which is 0.013/0.026 Å (Ru4/Ru4a). Overall, **3b** is a 68-electron cluster, electron precise for a four-metal cluster with two metal–metal bonds.

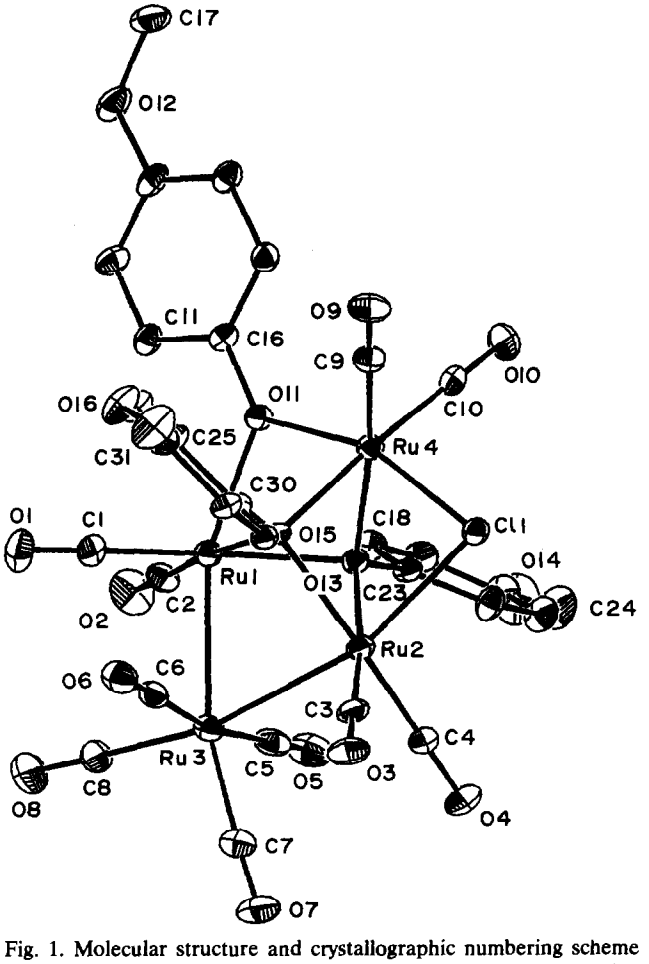

Fig. 1. Molecular structure and crystallographic numbering scheme for the two independent molecules of $Ru_4(\mu_3$-OC_6H_4OMe-4)$_2(\mu$-Cl)(μ-OC_6H_4OMe-4)$(CO)_{10}$ (**3b**); 20% thermal ellipsoids are shown for the non-hydrogen atoms. Hydrogen atoms have arbitrary radii of 0.1 Å.

TABLE 1. Summary of crystallographic data for $Ru_4(\mu_3$-OC_6H_4OMe-4)$_2(\mu$-Cl)(μ-OC_6H_4OMe-4)$(CO)_{10}$ (**3b**)

Formula	$C_{31}H_{21}ClNO_{16}Ru_4$
M (g mol^{-1})	1089.24
Crystal system	triclinic
Space group	$P\bar{1}$ (No. 2)
a (Å)	9.76(2)
b (Å)	17.52(2)
c (Å)	22.25(4)
α (°)	79.3(1)
β (°)	85.7(1)
γ (°)	89.6(1)
V (Å^3)	3726
Z	4
D_x (g cm^{-3})	2.01
μ_{Mo} (cm^{-1})	17.7
A^* min, max	1.00, 1.19
$F(000)$	2180
θ_{max} (°)	25
N	13071
N_O	8020
R	0.041
R_w	0.041
GOF	3.96

Our interest in this structure centres on the coordination of the bridging ligands. All four bridging ligands bridge asymmetrically; the (μ_3-OC_6H_4OMe-4) ligands have Ru(4)–O [av. 2.14 Å] substantially shorter than Ru(1)–O and Ru(2)–O [av. 2.20 Å], Ru(4)–O [2.04 Å] is significantly less than Ru(1)–O [2.23 Å] for (μ-OC_6H_4OMe-4) and Ru(4)–Cl [2.37 Å] is much less than Ru(2)–Cl [2.58 Å]. Taken together, these distances are suggestive of an interaction involving ruthenium in different oxidation states. The molecular geometry and asymmetry of the bridging ligands are similar to those of the structurally characterized analogues $Ru_4(\mu_3$-$OEt)_2(\mu$-$Cl)_2(CO)_{10}$ [10] and $Ru_4(\mu_3$-$OPh)_2(\mu$-$Cl)_2(CO)_{10}$ [11], the former obtained by reaction between $Ru_3(CO)_{12}$ and $[N(PPh_3)_2]Cl$ in EtOH, the latter by reaction between $Ru_3(CO)_{12}$, phenol and CCl_4 in cyclohexane. Recently, the related 'spiked triangular' cluster anion $[Ru_4(\mu$-$Cl)_2(CO)_{11}]^{2-}$ has been isolated and structurally characterized [12]; the

spiked $Ru(CO)_2(Cl)_2$ fragment is attached to the triangular $Ru_3(CO)_9$ unit by two asymmetrically bridging chloro ligands. As with **3b**, distances to the unique ruthenium (2.416(4), 2.417(4) Å) are significantly shorter than those to the triangular core rutheniums (2.536(4), 2.534(4) Å). Complex **3b** thus demonstrates that this structural motif is not restricted to μ-chloro ligands, the general features being retained on replacement of μ-chloro by μ-phenoxo.

As neither of the reagents nor solvent cyclohexane contain chlorine, attempts were made to ascertain its source. Complex **3c** as a precursor to **3b** was discounted following unsuccessful attempts at reaction of the former with dichloromethane in the presence of silica, typical reaction mixture chromatography conditions. We believe that the chlorine originates as carbon tetrachloride contaminant in the LR grade cyclohexane employed in the reaction; repeating the reaction with multiply distilled cyclohexane led to extremely low (0.7%) yields of **3b**. Attempted confirmation of the presence of carbon tetrachloride in the LR grade cyclohexane by GLC methods was unsuccessful, but the quantities of carbon tetrachloride required to afford yields of **3b** as in this reaction are below the detection limits of the GLC equipment employed. As $Ru_4(\mu_3\text{-}OPh)_2(\mu\text{-}Cl)_2(CO)_{10}$, an analogue of **3b**, was obtained from deliberate reaction between $Ru_3(CO)_{12}$, phenol and carbon tetrachloride in cyclohexane [11], we believe that the formation of **3b** and **4b** in our case is due to small amounts of CCl_4 accidentally contaminating the reaction solvent.

2.3. Dynamic NMR studies on 4c

The room-temperature ^{13}C NMR spectrum of **4c** shows broadened signals at 200.8, 161.6 and 110.7 ppm, corresponding to metal-bound carbonyl, and the *ipso* and *ortho* carbons of the organic ligands, respectively. Variable temperature NMR spectra of **4c** were recorded in an effort to elucidate the reason for this broadening, and are presented in Fig. 2.

As can be seen, the signal at 200.8 ppm decoalesces to give four CO resonances at 238 K assigned to the metal-bound carbonyls labelled d (Fig. 3), while the signal at 161.6 ppm decoalesces to three signals at the lower temperature to give a total of four signals in the ratio of 0.5:1:0.5:2 due to the *ipso* carbons. The signal at 110.7 ppm decoalesces to three signals in the ratio 1:2:1 at 238 K. Coalescence temperatures for these processes are 285 ± 2 K, 283 ± 2 K and 283 ± 2 K, respectively, although no attempt was made to calculate $\Delta G^{\neq}$ values for the three signals to prove that they arise from the same process. The occurrence of resonances corresponding to Ru–CO, C–O and C–H strongly suggests that the dynamic process is restricted rotation about an Ar–O bond.

The coalescing Ru–CO signals arise from the two equivalent $Ru(CO)_2$ groups; rapid rotation about the aryloxy C–O bonds would lead to equivalent signals (Fig. 3). It is also apparent from examination of the *ipso*-carbon signals that the low-energy conformations must have a plane of symmetry as the μ_3-naphthoxo C–O are equivalent at low temperature. This confirms that the dynamic process involves restricted rotation about the μ_2-naphthoxo C–O and suggests that the aromatic rings in the low-energy conformations are in the tetraruthenium plane; the low-energy conformations are presumably planar to maximize orbital overlap of the oxygen $2p_z$ with the π system of the naphthyl moiety. Rotation about the C–O bond in the μ_2 ligand is a higher energy process than that with the μ_3 ligand, as the former has a lone pair of electrons on the oxygen available for donation into the aromatic system, thus increasing the C–O bond order; with the latter, this electron pair ligates the third metal. These low-energy conformations would only be observable in **4c**. To confirm this, the low-temperature (228 K) ^{13}C NMR spectrum of **3c** was examined, and found to be identical to the spectrum acquired at 298 K, the result expected on the basis of the symmetry of the 4-methoxyphenoxo group.

2.4. Nature of the isomerism in raft clusters

Bhaduri and coworkers have reported that warming **2a** to 50°C caused no change in the hydrido ligand signals in the ^1H NMR spectrum. Warming **3a** to 90°C in toluene-d_8 caused broadening of the edge-bridging and the face-capping hydrido ligands. It has been suggested that the isomerism is associated with the hydrido ligand bridging differing Ru–Ru bonds [9], and the result here is consistent with the onset of exchange between the two edge-bridging hydrido ligand sites. Employing the higher boiling dimethylsulfoxide-d_6 to examine exchange of the edge-bridging and face-capping hydrides caused a reaction to take place, affording as yet uncharacterized products. An EXSY experiment at 70°C revealed cross peaks, suggesting that the edge-bridging and face-capping hydrido ligands would all exchange at the high-temperature limit. These experiments are consistent with the isomerism being associated with a hydrido ligand bridging differing edges. Increasing the temperature caused site-exchange of this hydride and removed the isomerism. We have recently found that deprotonation of this hydride followed by auration also removes the isomerism [13]. However, structural studies on raft clusters of this type have not thus far succeeded in identifying both isomers [7–9,13].

TABLE 2. Non-hydrogen atomic coordinates and equivalent isotropic thermal parameters for $Ru_4(\mu_3\text{-}OC_6H_4OMe\text{-}4)_2(\mu\text{-}Cl)(\mu\text{-}OC_6H_4OMe\text{-}4)(CO)_{10}$ (3b)

Atom	x	y		U_{eq} [a]
Ru(1)	0.60931(8)	0.04151(5)	0.26782(4)	0.0401(3)
Ru(2)	0.31081(8)	0.01143(4)	0.32840(4)	0.0397(3)
Ru(3)	0.53568(9)	−0.07515(5)	0.36565(4)	0.0461(3)
Ru(4)	0.37443(8)	0.14792(5)	0.21758(3)	0.0406(3)
Cl(1)	0.1562(3)	0.1155(2)	0.2701(1)	0.0471(9)
C(1)	0.723(1)	−0.0251(7)	0.2336(5)	0.058(4)
O(1)	0.797(1)	−0.0654(6)	0.2132(5)	0.093(4)
C(2)	0.758(1)	0.0634(6)	0.3069(5)	0.048(4)
O(2)	0.8486(8)	0.0740(6)	0.3332(4)	0.082(4)
C(3)	0.252(1)	0.0105(5)	0.4087(5)	0.042(3)
O(3)	0.2110(9)	0.0073(5)	0.4589(3)	0.067(3)
C(4)	0.209(1)	−0.0778(6)	0.3374(5)	0.052(4)
O(4)	0.149(1)	−0.1352(5)	0.3463(4)	0.079(4)
C(5)	0.567(1)	0.0025(6)	0.4157(4)	0.042(3)
O(5)	0.5859(9)	0.0458(4)	0.4454(3)	0.063(3)
C(6)	0.496(1)	−0.1353(6)	0.3032(5)	0.057(4)
O(6)	0.476(1)	−0.1696(5)	0.2665(4)	0.076(4)
C(7)	0.435(1)	−0.1466(6)	0.4309(5)	0.057(4)
O(7)	0.374(1)	−0.1872(5)	0.4684(4)	0.081(4)
C(8)	0.716(1)	−0.1174(6)	0.3772(5)	0.057(4)
O(8)	0.824(1)	−0.1409(6)	0.3836(5)	0.097(5)
C(9)	0.355(1)	0.2536(6)	0.2177(5)	0.046(4)
O(9)	0.341(1)	0.3170(4)	0.2200(4)	0.071(3)
C(10)	0.308(1)	0.1628(7)	0.1407(5)	0.051(4)
O(10)	0.266(1)	0.1697(6)	0.0941(4)	0.083(4)
O(11)	0.5798(7)	0.1433(4)	0.1934(3)	0.040(2)
O(12)	0.9433(8)	0.3226(5)	0.0239(4)	0.068(3)
C(11)	0.622(1)	0.2575(6)	0.1173(4)	0.043(4)
C(12)	0.714(1)	0.3042(6)	0.0737(5)	0.049(4)
C(13)	0.847(1)	0.2821(6)	0.0665(4)	0.046(4)
C(14)	0.891(1)	0.2149(7)	0.1025(5)	0.056(4)
C(15)	0.803(1)	0.1694(6)	0.1447(5)	0.045(4)
C(16)	0.666(1)	0.1894(6)	0.1524(4)	0.039(3)
C(17)	0.901(1)	0.3894(8)	−0.0157(6)	0.073(5)
O(13)	0.4489(6)	0.1118(3)	0.3067(3)	0.033(2)
O(14)	0.5511(8)	0.3537(5)	0.4254(4)	0.069(3)
C(18)	0.583(1)	0.2215(6)	0.3183(4)	0.041(3)
C(19)	0.603(1)	0.2811(6)	0.3481(5)	0.052(4)
C(20)	0.517(1)	0.2922(6)	0.3985(5)	0.047(4)
C(21)	0.408(1)	0.2425(6)	0.4183(5)	0.047(4)
C(22)	0.387(1)	0.1825(5)	0.3879(4)	0.039(3)
C(23)	0.475(1)	0.1726(5)	0.3388(4)	0.034(3)
C(24)	0.454(1)	0.3744(8)	0.4700(7)	0.081(6)
O(15)	0.4067(6)	0.0249(4)	0.2339(3)	0.038(2)
O(16)	0.263(1)	−0.1274(6)	0.0514(4)	0.096(5)
C(25)	0.470(1)	−0.0226(7)	0.1417(5)	0.052(4)
C(26)	0.437(1)	−0.0608(7)	0.0954(5)	0.061(5)
C(27)	0.308(1)	−0.0892(7)	0.0957(6)	0.067(5)
C(28)	0.207(1)	−0.0787(8)	0.1409(6)	0.074(6)
C(29)	0.242(1)	−0.0416(7)	0.1869(5)	0.056(4)
C(30)	0.372(1)	−0.0143(6)	0.1876(5)	0.043(4)
C(31)	0.360(2)	−0.140(1)	0.0042(8)	0.13(1)
Ru(1a)	0.11115(8)	0.56872(5)	0.26343(4)	0.0435(3)
Ru(2a)	−0.18605(8)	0.57250(5)	0.32488(4)	0.0426(3)
Ru(3a)	0.03939(9)	0.63898(5)	0.36205(4)	0.0497(3)
Ru(4a)	−0.12432(8)	0.48647(5)	0.21461(4)	0.0409(3)
Cl(1a)	−0.3413(3)	0.4960(2)	0.2679(1)	0.0469(9)
C(1a)	0.227(1)	0.6496(7)	0.2302(5)	0.055(4)
O(1a)	0.302(1)	0.6999(6)	0.2092(5)	0.093(4)
C(2a)	0.260(1)	0.5280(7)	0.3026(5)	0.050(4)
O(2a)	0.3508(8)	0.5023(6)	0.3294(4)	0.082(4)
C(3a)	−0.282(1)	0.6595(6)	0.3342(5)	0.056(4)
O(3a)	−0.346(1)	0.7127(5)	0.3424(5)	0.085(4)
C(4a)	−0.247(1)	0.5380(6)	0.4049(5)	0.053(4)
O(4a)	−0.2845(9)	0.5168(5)	0.4550(3)	0.070(3)
C(5a)	0.004(1)	0.7307(7)	0.3004(5)	0.059(4)
O(5a)	−0.018(1)	0.7834(5)	0.2648(4)	0.084(4)
C(6a)	0.069(1)	0.5383(7)	0.4124(5)	0.052(4)
O(6a)	0.0881(9)	0.4801(5)	0.4430(4)	0.068(3)
C(7a)	−0.058(1)	0.6796(7)	0.4287(5)	0.058(4)
O(7a)	−0.119(1)	0.7012(5)	0.4670(4)	0.081(4)
O(8a)	0.325(1)	0.6942(6)	0.3794(5)	0.099(5)
C(8a)	0.218(1)	0.6743(7)	0.3727(6)	0.061(5)
C(9a)	−0.143(1)	0.3795(6)	0.2172(4)	0.047(4)
O(9a)	−0.157(1)	0.3155(4)	0.2211(4)	0.069(3)
C(10a)	−0.193(1)	0.5020(6)	0.1378(5)	0.051(4)
O(10a)	−0.2370(9)	0.5130(5)	0.0916(4)	0.076(4)
O(11a)	0.0795(6)	0.5021(4)	0.1900(3)	0.041(2)
O(12a)	0.4404(8)	0.3957(5)	0.0199(4)	0.071(3)
C(11a)	0.122(1)	0.4203(6)	0.1139(5)	0.048(4)
C(12a)	0.211(1)	0.3918(6)	0.0721(5)	0.049(4)
C(13a)	0.344(1)	0.4178(6)	0.0626(5)	0.051(4)
C(14a)	0.389(1)	0.4715(7)	0.0953(6)	0.061(5)
C(15a)	0.301(1)	0.4983(6)	0.1379(5)	0.048(4)
C(16a)	0.167(1)	0.4731(5)	0.1470(4)	0.038(3)
C(17a)	0.402(2)	0.3401(8)	−0.0136(6)	0.081(6)
O(13a)	−0.0479(6)	0.4817(3)	0.3020(3)	0.036(2)
O(14a)	0.0507(8)	0.1836(4)	0.4255(4)	0.067(3)
C(18a)	0.087(1)	0.3653(6)	0.3173(5)	0.047(4)
C(19a)	0.107(1)	0.2908(6)	0.3479(5)	0.053(4)
C(20a)	0.019(1)	0.2582(6)	0.3972(5)	0.052(4)
C(21a)	−0.092(1)	0.2993(6)	0.4159(5)	0.046(4)
C(22a)	−0.113(1)	0.3740(5)	0.3842(4)	0.039(3)
C(23a)	−0.0262(9)	0.4065(5)	0.3362(4)	0.034(3)
C(24a)	−0.045(2)	0.1434(8)	0.4699(7)	0.086(6)
O(15a)	−0.0929(7)	0.6023(4)	0.2297(3)	0.041(2)
O(16a)	−0.240(1)	0.8587(6)	0.0607(4)	0.093(4)
C(25a)	−0.261(1)	0.6925(7)	0.1848(5)	0.057(4)
C(26a)	−0.297(1)	0.7566(7)	0.1421(6)	0.066(5)
C(27a)	−0.195(1)	0.7940(7)	0.1004(5)	0.061(5)
C(28a)	−0.063(1)	0.7669(7)	0.0995(5)	0.061(4)
C(29a)	−0.029(1)	0.7017(6)	0.1425(5)	0.052(4)
C(30a)	−0.128(1)	0.6668(6)	0.1848(5)	0.042(3)
C(31a)	−0.138(2)	0.9056(9)	0.0239(8)	0.111(8)

[a] Equivalent isotropic U defined as one-third of the trace of the orthogonalized U_{ij} tensor.

2.5. *Implications for hydrodeoxygenation modelling*

Our primary motivation for examining the reactions of substituted phenols with **1** was to afford model compounds for hydrodeoxygenation, and the work described above gave products with phenoxo ligands in various coordination modes. The μ_5-η^7-bound phenoxo ligands on raft clusters such as **(2–4)a** would seem good models for surface-coordinated and -activated phenol; indeed, phenol has recently been imaged on the $TiO_2(110)$ surface by STM and shown to (i) coordinate parallel to the surface and (ii) induce surface puckering suggesting a similar coordination geometry

TABLE 3. Selected bond and contact lengths (Å) for $Ru_4(\mu_3\text{-}OC_6H_4OMe\text{-}4)_2(\mu\text{-}Cl)(\mu\text{-}OC_6H_4OMe\text{-}4)(CO)_{10}$ (**3b**) [a]

Ru(1)···Ru(2)	3.121(5), 3.117(5)	Ru(1)–Ru(3)	2.749(3), 2.753(3)
Ru(1)···Ru(4)	3.088(3), 3.088(3)	Ru(2)–Ru(3)	2.751(3), 2.747(3)
Ru(2)···Ru(4)	3.127(3), 3.129(4)	Ru(1)–O(11)	2.230(6), 2.218(7)
Ru(1)–O(13)	2.208(6), 2.194(6)	Ru(1)–O(15)	2.209(7), 2.218(7)
Ru(2)–O(13)	2.181(6), 2.185(6)	Ru(2)–O(15)	2.207(7), 2.211(7)
Ru(2)–Cl(1)	2.581(3), 2.579(4)	Ru(4)–O(11)	2.041(7), 2.029(7)
Ru(4)–O(13)	2.145(6), 2.121(7)	Ru(4)–O(15)	2.144(7), 2.145(7)
Ru(4)–Cl(1)	2.370(4), 2.367(4)	O(13)···O(15)	2.48(1), 2.464(8)
Ru(1)–C(1)	1.83(3), 1.83(1)	Ru(1)–C(2)	1.82(1), 1.82(1)
Ru(2)–C(3)	1.83(1), 1.82(1)	Ru(2)–C(4)	1.83(1), 1.83(1)
Ru(3)–C(5)	1.95(1), 1.96(1)	Ru(3)–C(6)	1.96(1), 1.94(1)
Ru(3)–C(7)	1.94(1), 1.94(1)	Ru(3)–C(8)	1.92(1), 1.90(1)
Ru(4)–C(9)	1.86(1), 1.87(1)	Ru(4)–C(10)	1.85(1), 1.85(1)
C(1)–O(1)	1.13(2), 1.16(1)	C(2)–O(2)	1.13(1), 1.15(1)
C(3)–O(3)	1.15(1), 1.15(1)	C(4)–O(4)	1.15(1), 1.14(1)
C(5)–O(5)	1.12(1), 1.13(1)	C(6)–O(6)	1.13(2), 1.14(1)
C(7)–O(7)	1.12(1), 1.12(1)	C(8)–O(8)	1.14(2), 1.13(2)
C(9)–O(9)	1.13(1), 1.12(1)	C(10)–O(10)	1.13(1), 1.13(1)
O(11)–C(16)	1.35(1), 1.40(1)	O(13)–C(23)	1.42(1), 1.42(1)
O(15)–C(30)	1.40(1), 1.42(1)	C(11)–C(16)	1.38(1), 1.38(2)
C(11)–C(12)	1.41(1), 1.39(2)	C(12)–C(13)	1.35(2), 1.36(2)
C(13)–C(14)	1.38(1), 1.38(2)	C(14)–C(15)	1.36(1), 1.38(2)
C(15)–C(16)	1.38(1), 1.36(1)	C(13)–O(12)	1.38(1), 1.39(1)
O(12)–C(17)	1.41(1), 1.40(2)	C(23)–C(18)	1.36(1), 1.39(1)
C(18)–C(19)	1.36(2), 1.38(1)	C(19)–C(20)	1.39(2), 1.37(1)
C(20)–C(21)	1.37(1), 1.38(2)	C(21)–C(22)	1.38(2), 1.39(1)
C(22)–C(23)	1.37(1), 1.35(1)	C(20)–O(14)	1.38(1), 1.38(1)
O(14)–C(24)	1.41(2), 1.40(2)	C(30)–C(25)	1.37(1), 1.37(2)
C(25)–C(26)	1.39(2), 1.39(2)	C(26)–C(27)	1.36(2), 1.39(2)
C(27)–C(28)	1.39(2), 1.36(2)	C(28)–C(29)	1.37(2), 1.40(1)
C(29)–C(30)	1.37(2), 1.36(1)	C(27)–O(16)	1.39(2), 1.39(1)
O(16)–C(31)	1.41(2), 1.41(2)		

[a] Two values refer to two molecules in the asymmetric unit.

TABLE 4. Selected bond angles (°) for $Ru_4(\mu_3\text{-}OC_6H_4OMe\text{-}4)_2(\mu\text{-}Cl)(\mu\text{-}OC_6H_4OMe\text{-}4)(CO)_{10}$ (**3b**) [a]

Ru(1)–Ru(3)–Ru(2)	69.2(1), 69.05(9)	Ru(3)–Ru(1)–O(11)	157.2(2), 156.9(2)
Ru(3)–Ru(2)–Cl(1)	162.53(7), 162.60(7)	Ru(3)–Ru(1)–O(13)	86.5(2), 86.6(2)
Ru(3)–Ru(2)–O(13)	87.0(2), 86.9(2)	Ru(3)–Ru(2)–O(15)	87.3(2), 88.1(2)
Ru(3)–Ru(1)–O(15)	87.3(2), 87.8(2)	O(11)–Ru(4)–O(13)	80.3(3), 79.8(3)
O(11)–Ru(4)–O(15)	79.0(3), 78.6(3)	O(13)–Ru(1)–O(15)	68.2(3), 67.9(2)
O(13)–Ru(2)–O(15)	68.7(2), 68.2(2)	Cl(1)–Ru(2)–O(15)	78.6(2), 78.3(2)
O(15)–Ru(4)–Cl(1)	84.7(2), 84.5(2)	O(11)–Ru(1)–O(13)	75.0(2), 74.3(2)
O(11)–Ru(1)–O(15)	73.7(2), 73.2(3)	O(11)–Ru(4)–Cl(1)	160.4(2), 159.8(2)
O(13)–Ru(4)–O(15)	70.5(2), 70.6(2)	O(13)–Ru(2)–Cl(1)	78.4(2), 78.0(2)
O(13)–Ru(4)–Cl(1)	84.0(2), 84.2(2)	Ru(2)–O(13)–Ru(1)	90.6(2), 90.8(2)
Ru(2)–O(15)–Ru(1)	90.0(3), 89.5(3)	Ru(1)–O(11)–Ru(4)	92.5(3), 93.2(3)
Ru(1)–O(15)–Ru(4)	90.4(3), 90.1(3)	Ru(1)–O(13)–Ru(4)	90.3(2), 91.4(2)
Ru(2)–Cl(1)–Ru(4)	78.2(1), 78.3(1)	Ru(2)–O(13)–Ru(4)	92.6(3), 93.2(2)
Ru(2)–O(15)–Ru(4)	91.9(3), 91.8(2)	Ru(1)–O(11)–C(16)	133.8(6), 134.1(6)
Ru(1)–O(13)–C(23)	124.9(5), 126.3(5)	Ru(1)–O(15)–C(30)	129.7(6), 129.1(6)
Ru(2)–O(13)–C(23)	132.1(5), 129.0(5)	Ru(2)–O(15)–C(30)	127.7(5), 125.8(6)
Ru(4)–O(11)–C(16)	133.4(6), 132.3(6)	Ru(4)–O(13)–C(23)	115.6(5), 116.06(7)
Ru(4)–O(15)–C(30)	116.4(5), 119.8(6)	C(13)–O(12)–C(17)	118.3(9), 119(1)
C(20)–O(14)–C(24)	117.1(9), 118.2(9)	C(27)–O(16)–C(31)	117(1), 116(1)

[a] Two values refer to two molecules in the asymmetric unit.

to that observed in the raft clusters [14]. However, carbonylation of **2a** is reported to regenerate **1** [9], and hydrogenation (1 atm H_2, refluxing benzene, 16 h) of **3a** affords $Ru_4(\mu\text{-}H)_4(CO)_{12}$ as the major product [13]; for the latter reaction, no organic byproducts have thus far been identified. Further work aimed at reducing **3a** under mild conditions is currently underway.

Hydrotreating catalysts typically couple early and late transition metals (*e.g.* the commercial Co–Mo catalyst supported on alumina). The nature of the active site in such catalysts is not clear, but may involve the disparate metals in close proximity. Complexes such as **3b,c** and **4b,c** could thus be considered to model phenols absorbed on hydrotreating catalysts, where the high oxidation state ruthenium models the oxophilic early transition metal.

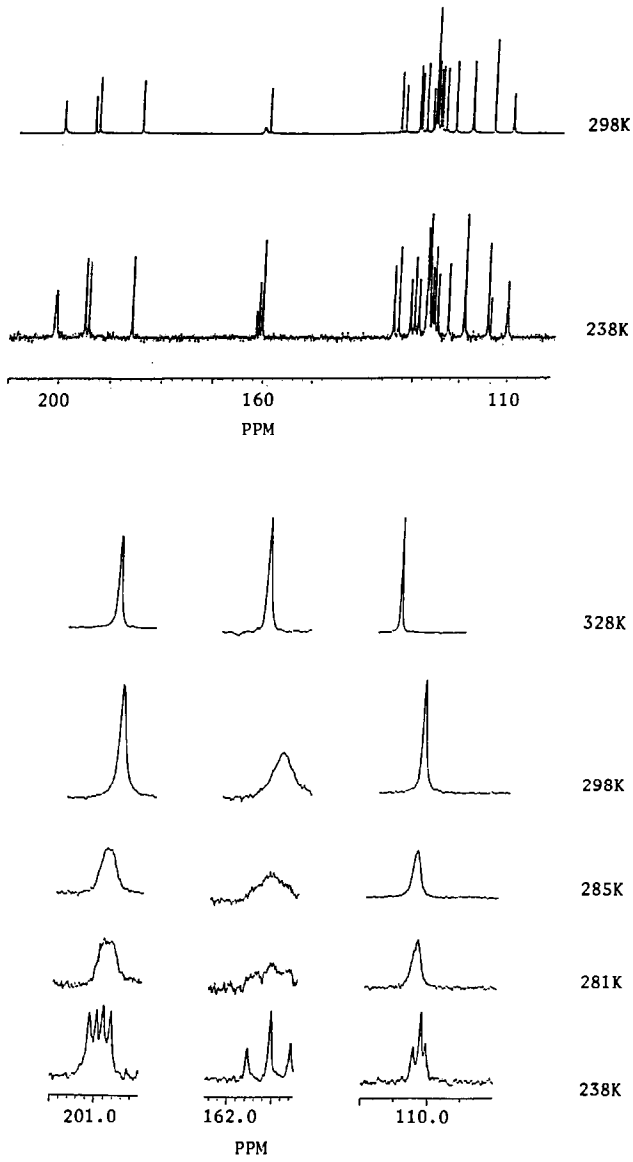

Fig. 2. Dynamic ^{13}C NMR spectra for $Ru_4(\mu_3\text{-}OC_{10}H_7)_2(\mu\text{-}OC_{10}H_7)_2(CO)_{10}$ (**4c**).

3. Experimental details

$Ru_3(CO)_{12}$ was synthesized from $RuCl_3$ as previously described [15]. 4-Methoxyphenol, 2-naphthol, 3,5-dimethylphenol, 1-naphthol (BDH) and 4-ethylphenol (Koch–Light Laboratories) were obtained commercially and recrystallized from CH_2Cl_2/hexane before use. The cyclohexane was routinely LR grade (Ajax) and dried over sodium wire, except where efforts to identify the source of the chlorine in **3b** and **4b** were made when high-purity, redistilled cyclohexane was used. The reactions were carried out using standard Schlenk techniques [16] under dry argon or nitrogen, although subsequent work-up was carried out without any precautions to exclude air. Column chromatography was performed on 35–70 mesh May&Baker silica and thin layer chromatography was carried out on glass plates (20 × 20 cm) coated with Merck Kieselgel 60 GF_{254} silica gel (0.5 mm). Eluate mixtures were diluted with light petroleum of boiling point range 60–70°C. The known complexes were identified by comparison of their IR and NMR spectra with the literature values.

IR spectra were recorded using a Perkin-Elmer model 1725 Fourier transform spectrophotometer with CaF_2 optics. NMR spectra were recorded on a Bruker AM300 spectrometer, the ^1H spectra at 300.13 MHz, the ^{13}C at 75.47 MHz using approximately 0.02 M $Cr(acac)_3$ as the relaxation agent and a recycle delay of 0.5 s. FAB mass spectra were recorded using a VG ZAB 2HF instrument (exciting gas Ar, source pressure 10^{-6} mbar, FAB gun voltage 7.5 kV, current 1 mA, accelerating potential 8 kV) at the University of Adelaide. The matrix was 3-nitrobenzyl alcohol. Peaks were recorded as m/z values. GC analyses were carried out on a Varian 3300 gas chromatograph. Elemental microanalyses were by Dr. O. b. Shawkataly at the Universiti Sains Malaysia, Penang, Malaysia or Dr. N. Jacobsen at the Microanalytical Service at the Department of Chemistry, University of Queensland.

3.1. Reaction between $Ru_3(CO)_{12}$ and 4-methoxyphenol

A mixture consisting of $Ru_3(CO)_{12}$ (500 mg, 0.782 mmol) and 4-methoxyphenol (971 mg, 7.82 mmol) in cyclohexane (30 ml) was refluxed for 4 d. The resulting deep red solution was taken to dryness and subjected to column chromatography. Elution with light petroleum afforded a mixture of $Ru_4(\mu\text{-}H)_4(CO)_{12}$ (40 mg, 9%), unchanged $Ru_3(CO)_{12}$ (15 mg, 3%) and $Ru_4(\mu\text{-}H)_2(CO)_{13}$ (10 mg, 2%). Elution with 33%

CH_2Cl_2 gave a dark purple band, the product from which was crystallized from CH_2Cl_2/hexane to afford $Ru_6(\mu\text{-}H)_2(\mu_5\text{-}\eta^7\text{-}OC_6H_3OMe\text{-}4)(CO)_{16}$ (**3a**; 156 mg, 35%, m.p. > 360°C). Elution with 50% CH_2Cl_2 gave a yellow/orange band, the product from which was crystallized from CH_2Cl_2/MeOH to afford $Ru_4(\mu_3\text{-}OC_6H_4OMe\text{-}4)_2(\mu\text{-}Cl)(\mu\text{-}OC_6H_4OMe\text{-}4)(CO)_{10}$ (**3b**; 26 mg, 4%, m.p. 169–172°C (dec.)). Elution with 65% CH_2Cl_2 gave a yellow/orange band the product from which was crystallized from n-heptane to afford $Ru_4(\mu_3\text{-}OC_6H_4OMe\text{-}4)_2(\mu\text{-}OC_6H_4OMe\text{-}4)_2(CO)_{10}$ (**3c**; 24 mg, 4%). Elution with methanol gave a deep red solution from which $[NEt_4][Ru_6(\mu_6\text{-}H)(CO)_{18}]$ (8 mg, 1%) was isolated following metathesis with $[NEt_4]Br$.

Complex **3a**: Analysis: Found: C, 23.02; H, 0.43%; M^+ 1179. $C_{23}H_8O_{18}Ru_6$ requires: C, 23.42; H, 0.63%; M^+ 1179. IR (cyclohexane) (cm^{-1}): 2113 (m); 2100 (m); 2075 (s); 2051 (s, sh); 2047 (vs); 2041 (s); 2028 (s); 2024 (s); 2013 (s); 1966 (m); 1811 (m). ^1H NMR ($CDCl_3$) δ: Major isomer: 6.61 (dd, J(HH) = 3 Hz, 6 Hz, 1H, H3); 4.06 (d, J(HH) = 3 Hz, 1H, H2); 3.69 (s, 3H, OCH_3); 3.43 (d, J(HH) = 6 Hz, 1H, H5); −11.88 (s, 1H, Ru–H); −21.86 (s, 1H, Ru–H) ppm. Minor isomer: 6.43 (dd, J(HH) = 3 Hz, 6 Hz, 1H, H3); 4.01 (d, J(HH) = 3 Hz, 1H, H2); 3.84 (d, J(HH) = 6 Hz, 1H, H5); 3.70 (s, 3H, OCH_3); −12.72 (s, 1H, Ru–H); −22.36 (s, 1H, Ru–H) ppm. ^{13}C NMR (acetone-d_6) δ: 209.5, 203.5, 203.3, 202.4, 200.8, 199.2, 199.0, 198.1, 196.4, 195.9, 195.7, 192.4, 190.4, 185.0, 183.3 (CO) ppm. ^{13}C NMR ($CDCl_3$) δ: 129.0, 128.2, 102.2, 96.0, 83.1, 79.9 (aryl C); 57.8, 57.5 (OCH_3) ppm.

Complex **3b**: Analysis Found: C, 34.14; H, 1.64%; M^+ 1090. $C_{31}H_{21}ClO_{16}Ru_4$ requires: C, 34.13; H, 1.94%; M^+ 1090. IR (cyclohexane) (cm^{-1}): 2105 (s); 2070 (s); 2041 (s); 2035 (s); 2027 (vs); 2010 (s); 1999 (m), 1955 (s); 1950 (s). ^1H NMR ($CDCl_3$) δ: 7.82 (m, 4H, o-H of μ_3-phenoxy); 6.95 (m, 4H, m-H of μ_3-phenoxy); 6.79 (m, 4H, aryl-H of μ_2-phenoxy); 3.84 (s, 6H, OCH_3); 3.80 (s, 3H, OCH_3) ppm. ^{13}C NMR ($CDCl_3$) δ: 200.9,

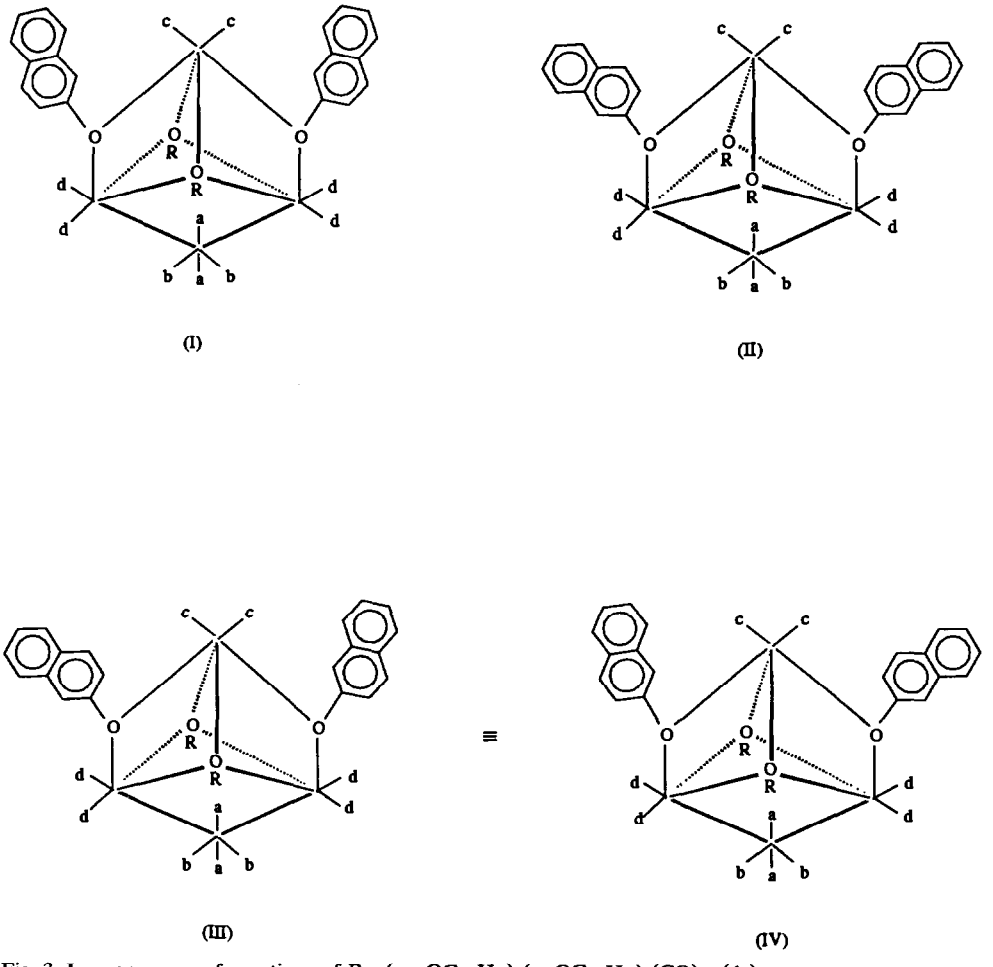

Fig. 3. Low-energy conformations of $Ru_4(\mu_3\text{-}OC_{10}H_7)_2(\mu\text{-}OC_{10}H_7)_2(CO)_{10}$ (**4c**).

199.9, 195.4, 192.6, 186.6, 186.0 (2:2:2:2:1:1, CO); 157.6, 155.9, 152.8 (*ipso*-C); 119.7, 116.7, 114.6, 114.3, (aryl C); 55.6, 55.4 (1:2, OCH_3) ppm.

Complex **3c**: Analysis: Found: C, 38.82; H, 2.42%; M^+ 1178. $C_{38}H_{28}O_{18}Ru_4$ requires: C, 38.72; H, 2.39%; M^+ 1178. IR (cyclohexane) (cm^{-1}): 2104 (s); 2061 (s); 2039 (s); 2034 (s); 2025 (vs); 2015 (w); 1997 (s); 1949 (s). ^1H NMR ($CDCl_3$) δ: 7.64 (m, 4H, *o*-H of μ_3-phenoxy); 6.85 (m, 4H, *m*-H of μ_3-phenoxy); 6.75 (m, 8H, aryl H of μ_2-phenoxy); 3.80, 3.79 (2 × s, 12H, OCH_3) ppm. ^{13}C NMR ($CDCl_3$) δ: 201.1, 195.3, 194.5, 186.7 (4:2:2:2, CO); 158.4, 157.4, 155.8, 152.6 (*ipso*-C); 119.4, 116.9, 114.6, 114.3 (aryl C); 55.6, 55.4, (OCH_3) ppm.

3.2. Reaction between $Ru_3(CO)_{12}$ and 2-naphthol

A mixture consisting of $Ru_3(CO)_{12}$ (500 mg, 0.782 mmol) and 2-naphthol (1.128 g, 7.82 mmol) was heated in refluxing cyclohexane (50 ml) for 60 h. The resulting deep red solution was taken to dryness and subjected to column chromatography. Elution with light petroleum afforded $Ru_4(\mu\text{-}H)_4(CO)_{12}$ (126 mg, 29%). Elution with 10% CH_2Cl_2 gave $Ru_4(\mu\text{-}H)_2(CO)_{13}$ (3 mg, 1%). Elution with 15% CH_2Cl_2 gave a mixture of two products which were separated by thin layer chromatography with 13% CH_2Cl_2 as eluent. The first band afforded a yellow powder from CH_2Cl_2/hexane identified as $Ru_4(\mu_3\text{-}OC_{10}H_7)_2(\mu\text{-}Cl)(\mu\text{-}OC_{10}H_7)(CO)_{10}$ (**4b**; 51 mg, 8%). Crystallization of the product from the second band from CH_2Cl_2/MeOH yielded orange crystals of $Ru_4(\mu_3\text{-}OC_{10}H_7)_2(\mu\text{-}OC_{10}H_7)_2(CO)_{10}$ (**4c**; 46 mg, 10%). Elution of the column with 50% CH_2Cl_2 gave a dark red band, the product from which was crystallized from CH_2Cl_2/hexane to give red–black crystals of $Ru_6(\mu\text{-}H)_2(\mu_5\text{-}\eta^7\text{-}OC_{10}H_6)(CO)_{16}$ (**4a**; 46 mg, 10%, m.p. > 350°C).

Complex **4a**: Analysis Found: C, 25.54; H, 0.69%; M^+ 1199. $C_{26}H_8O_{17}Ru_6$ requires: C, 26.04; H, 0.67%; M^+ 1199. IR (cyclohexane) (cm^{-1}): 2113 (m); 2100 (w); 2082 (w, sh); 2075 (s); 2052 (m, sh); 2047 (s); 2041 (s); 2029 (m); 2024 (m); 2015 (m); 1999 (m); 1980 (w); 1971 (m); 1948 (m); 1808 (w). ^1H NMR ($CDCl_3$) δ: Major isomer: 7.84–7.63, 7.45 (2 × m, 4H, 1H, H5–8); 5.04, 4.56 (2 × s, 2 × 1H, H1, H4); −11.68 (s, 1H, Ru–H); −21.07 (s, 1H, Ru–H) ppm. Minor isomer: 7.84–7.19, 7.45 (2 × m, 4H, 1H, H5–8); 4.93, 4.81 (2 × s, 2 × 1H, H1, H4); −12.55 (s, 1H, Ru–H); −21.23 (s, 1H, Ru–H) ppm. ^{13}C NMR ($CDCl_3$) δ: Two isomers: 207.0, 199.2, 198.5, 197.9, 197.2, 196.3, 195.8, 195.4 (CO); 139.4, 132.4, 131.7, 130.7, 130.2, 127.6, 127.1, 125.5, 113.3, 110.3, 102.2 (aromatic) ppm.

Complex **4b**: Analysis: Found: M^+ 1150. $C_{40}H_{21}ClO_{13}Ru_4$ requires: M^+ 1150. IR (cyclohexane) (cm^{-1}): 2107 (s); 2098 (w); 2080 (vw); 2073 (s); 2066 (w); 2043 (s); 2036 (vs); 2029 (vs); 2014 (s); 2001 (m); 1984 (vw,br); 1957 (s); 1953 (s); 1926 (vw, br). ^1H NMR ($CDCl_3$) δ: 8.38, 7.91–7.00 (s, m, 21H, $C_{10}H_7$) ppm. ^{13}C NMR ($CDCl_3$) δ: 200.7, 199.9, 195.2, 192.3, 186.2, 185.6 (2:2:2:2:1:1, CO); 161.0, 153.6 (*ipso*-C); 134.6, 134.3, 133.5, 130.6, 130.4, 129.7, 129.4, 128.5, 128.2, 127.6, 127.5, 127.4, 127.0, 126.5, 126.3, 126.1, 125.2, 123.2, 123.1, 119.7, 119.5, 118.9, 115.1, 111.4 (aryl C) ppm.

Complex **4c**: Analysis: Found: C, 47.00; H, 1.94%; M^+ 1258. $C_{50}H_{28}O_{14}Ru_4$ requires: C, 47.71; H, 2.24%; M^+ 1259. IR (cyclohexane) (cm^{-1}): 2107 (s); 2097 (w); 2065 (s); 2042 (s); 2036 (vs); 2028 (vs); 2016 (w); 2010 (vw); 2003 (s); 1999 (m); 1990 (w, sh, br). ^1H NMR ($CDCl_3$) δ: 8.24 (d, J(HH) = 2 Hz, 2H, H1); 7.96 (dd, J(HH) = 6 Hz, 2 Hz, 2H, H3); 7.88–7.80 (m, 8H); 7.75–7.69 (m, 4H); 7.48–7.31 (m, 10H); 7.09 (s, 2H); (naphthyl H) ppm. ^{13}C NMR (CD_2Cl_2) 298 K δ: 200.8, 194.9, 194.1, 185.9 (4:2:2:2, CO); 161.6, 160.6 (*ipso*-C); 134.3, 133.4, 130.6, 129.2, 127.9, 127.4, 127.2, 126.8, 126.4, 125.9, 125.0, 123.0, 119.3, 119.1, 114.6, 110.7 (aryl C) ppm. ^{13}C NMR (CD_2Cl_2) 238 K δ: 201.8, 201.6, 201.5, 201.3, 195.8, 195.1, 186.6 (1:1:1:1:2:2:2, CO); 162.2, 161.7, 161.2, 161.0 (*ipso*-C); 134.7, 133.7, 131.3, 130.5, 129.7, 128.2, 128.0, 127.7, 127.5, 126.9, 126.4, 125.7, 123.4, 119.9, 114.9, 111.1, 110.9, 110.7 (aryl C) ppm.

3.3. Reaction between $Ru_3(CO)_{12}$ and other substituted phenols

3.3.1. 1-Naphthol

A mixture consisting of $Ru_3(CO)_{12}$ (120 mg, 0.188 mmol) and 1-naphthol (270 mg, 1.88 mmol) was heated in refluxing cyclohexane (10 ml) for 3 d, after which time the solvent was removed and a CH_2Cl_2 extract of the residue subjected to column chromatography. Elution with hexane afforded $Ru_4(\mu\text{-}H)_4(CO)_{12}$ (17 mg, 16%), and elution with 20% CH_2Cl_2 gave $Ru_4(\mu\text{-}H)_2(CO)_{13}$ (9 mg, 8%). No other tractable products were obtained.

3.3.2. 4-Ethylphenol

Following the same procedure, $Ru_3(CO)_{12}$ (120 mg, 0.188 mmol) and 4-ethylphenol (229 mg, 1.88 mmol) in refluxing cyclohexane (20 ml) for 3 d afforded $Ru_4(\mu\text{-}H)_4(CO)_{12}$ (28 mg, 20%). No other tractable products were obtained.

3.3.3. 3,5-Dimethylphenol

Following the same procedure, $Ru_3(CO)_{12}$ (120 mg, 0.188 mmol) and 3,5-dimethylphenol (46 mg, 0.38 mmol) in refluxing cyclohexane (20 ml) for 4 d afforded successively unchanged $Ru_3(CO)_{12}$ (20 mg, 17%), $Ru_4(\mu\text{-}$

$H)_4(CO)_{12}$ (10 mg, 11%) and $Ru_4(\mu\text{-}H)_2(CO)_{13}$ (12 mg, 13%) after column chromatography. No other tractable products were obtained.

3.4. Structure determination

Intensity data for **2b** were collected at room temperature on an Enraf-Nonius CAD4F diffractometer. The unique diffractometer data set (ω–$1/3\theta$ scan mode; monochromatic Mo Kα radiation, $\lambda = 0.710693$ Å) was measured within the limits $1.2 < \theta < 25.0°$ at 297 K, yielding 13071 independent reflections; 8020 of these with $I \geq 2.5\sigma(I)$ were considered 'observed' and used in the block-diagonal least-squares refinements, after corrections were applied for Lorentz and polarization effects and for absorption correction, the latter using an empirical procedure based on Ψ-scans. The structure was solved by direct methods. Anisotropic thermal parameters were refined for the non-hydrogen atoms; the form of the isotropic and anisotropic temperature factors in the structure factor expression are $t = \exp(-8\pi^2 U s^2)$ and $t = \exp(-8\pi^2 U s^2(U_{11}h^2a^{*2} + \ldots + U_{23}klb^*c^*))$, respectively; $(x, y, z, U_{iso})_H$ were included constrained at estimated values. Conventional residuals R and R_w on $|F|$ are quoted at convergence. Neutral atom complex scattering factors were employed; computation used the XTAL 3.0 program system [17]. Pertinent results are given in Fig. 1 and the tables. Further details on the structural investigation are available from G.A.K. and C.L.R. Complete lists of atomic coordinates and thermal parameters, bond and contact lengths, and bond angles, have been deposited with the Cambridge Crystallographic Data Centre, 12 Union Road, Cambridge, CB2 1E2, UK. They may be obtained on request from the Director by citing the full literature reference for this paper.

Acknowledgements

We thank the Australian Research Council for support of this work, Johnson-Matthey Technology Centre for the loan of ruthenium salts, Mr. K. Byriel (University of Queensland) for the X-ray data collection, Mr. J.J. Campbell for preliminary experiments and Associate Professor S.R. Hall for helpful discussions regarding the XTAL 3.0 suite of programs. T.P.J. was the recipient of a UNE Vacation Research Scholarship. M.P.C. holds a UNE Postgraduate Research Scholarship.

References

1 M.I. Bruce, M.G. Humphrey, M.R. Snow, E.R.T. Tiekink and R.C. Wallis, *J. Organomet. Chem., 314* (1986) 311.
2 M.P. Cifuentes, M.G. Humphrey, B.W. Skelton and A.H. White, *J. Organomet. Chem., 466* (1994) 211.
3 M.P. Cifuentes, M.G. Humphrey, B.W. Skelton and A.H. White, *J. Organomet. Chem., 458* (1993) 211.
4 E. Furimsky, *Catal. Rev.-Sci. Eng., 25* (1983) 421.
5 M.I. Bruce, in G. Wilkinson, F.G.A. Stone and E.W. Abel (eds.), *Comprehensive Organometallic Chemistry*, Pergamon, Oxford, 1982, Vol. 4, pp. 880–881.
6 G. Lavigne, in D.F. Shriver, H.D. Kaesz and R.D. Adams (eds.), *The Chemistry of Metal Cluster Complexes*, VCH, New York, 1990, pp. 259–262.
7 S. Bhaduri, K.R. Sharma and P.G. Jones, *J. Chem. Soc., Chem. Commun.*, (1987) 1769.
8 H. Vahrenkamp and D.S. Bohle, *Angew. Chem., Int. Ed. Engl., 29* (1990) 198.
9 S. Bhaduri, K. Sharma, H. Khwaja and P.G. Jones, *J. Organomet. Chem., 412* (1991) 169.
10 B.F.G. Johnson, J. Lewis, J.M. Mace, P.R. Raithby and M.D. Vargas, *J. Organomet. Chem., 321* (1987) 409.
11 S. Bhaduri, N. Sapre, K. Sharma, P.G. Jones and G. Carpenter, *J. Chem. Soc., Dalton Trans.*, (1990) 1305.
12 G. Lavigne, N. Lugan, P. Kalck, J.M. Soulié, O. Lerouge, J.Y. Saillard and J.F. Halet, *J. Am. Chem. Soc., 114* (1992) 10669.
13 M.P. Cifuentes, T.P. Jeynes, M.G. Humphrey, B.W. Skelton and A.H. White, *J. Chem. Soc., Dalton Trans.*, (1994) 925.
14 K. Sakamaki, S. Matsunaga, K. Itoh, A. Fujishima and Y. Gohshi, *Surf. Sci., 219* (1989) L531.
15 M.I. Bruce, C.M. Jensen and N.L. Jones, *Inorg. Synth., 26* (1989) 259.
16 D.F. Shriver and M.A. Drezdzon, *The Manipulation of Air Sensitive Compounds*, 2nd edn., Wiley, New York, 1986.
17 S.R. Hall and J.M. Stewart (eds.), *The XTAL 3.0 Reference Manual*, Universities of Western Australia and Maryland, 1990.